Supporting information for:

MnO_x loaded mesoporous silica for the catalytic oxidation of formaldehyde. Effect of the melt infiltration conditions on the activity – stability behavior

Guillaume Rochard,[a] Carmen Ciotonea,[a] Adrian Ungureanu,*[b] Jean-Marc Giraudon,[a] Sébastien Royer,[a] Jean-François Lamonier*[a]

Graphical Abstract :

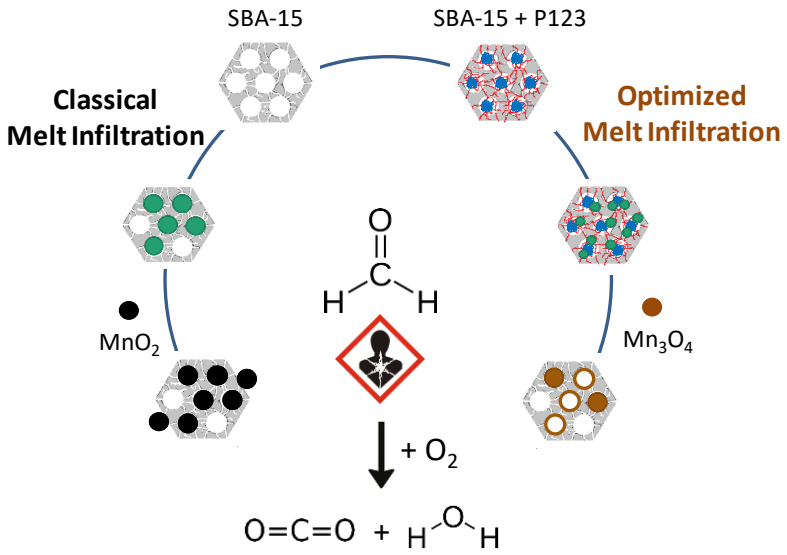

[a] G. Rochard, Dr. C. Ciotonea, Prof S. Royer, Dr. J.-M. Giraudon, Prof. J.-F. Lamonier
Univ. Lille, CNRS, ENSCL, Centrale Lille, Univ. Artois, UMR 8181 - UCCS - Unité de Catalyse et de Chimie du Solide, F-59000 Lille, France
E-mail: jean-francois.lamonier@univ-lille.fr

[b] Prof. A. Ungureanu
"Gheorghe Asachi" Technical University of Iasi, Faculty of Chemical Engineering and Environmental Protection, 73 D. Mangeron Bvd., 700050 Iasi, Romania.
E-mail: aungureanu@tuiasi.ro

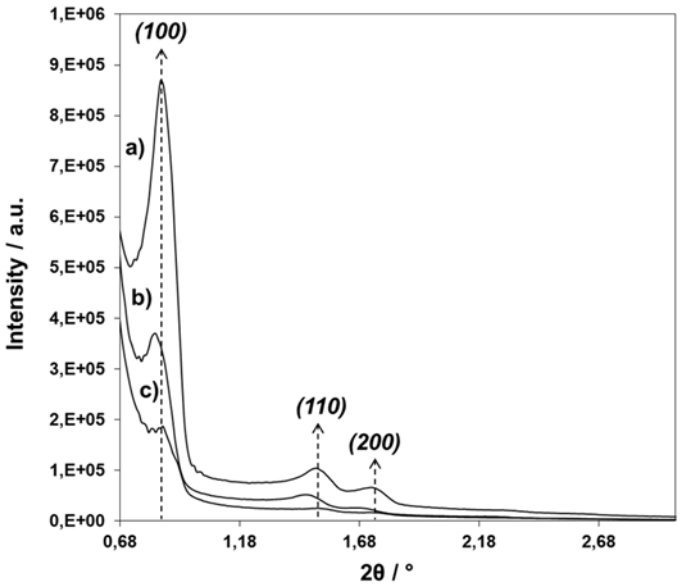

Figure S1. Low-angle XRD patterns for (a) SBA-15, (b) 20Mn-MIc300 and (c) 20Mn-MIa300

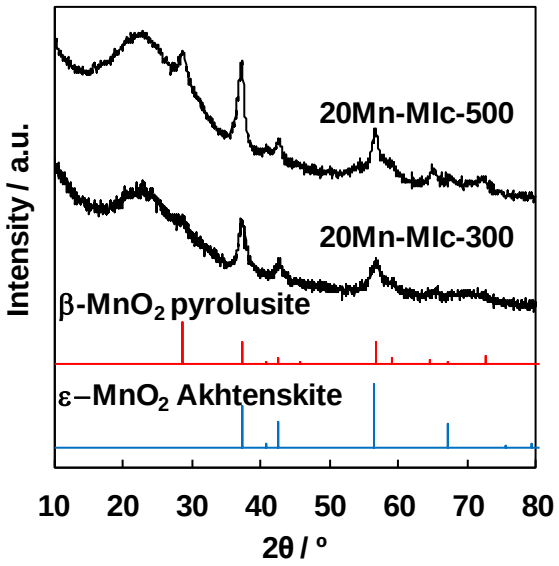

Figure S2. Wide-angle XRD patterns for 20Mn-MIc calcined at different temperatures

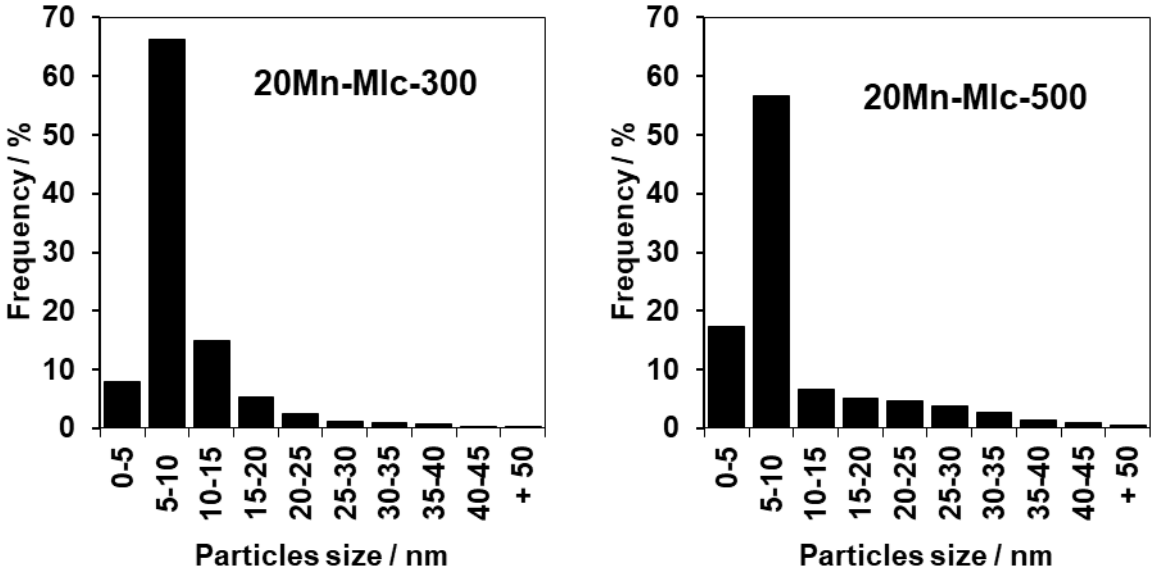

Figure S3. Particles size distribution for 20Mn-MIc calcined at different temperatures

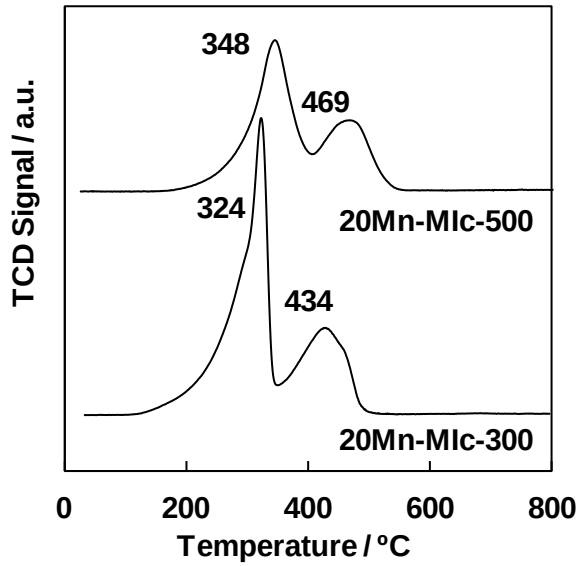

Figure S4. H_2-TPR profiles for 20Mn-MIc calcined at different temperatures

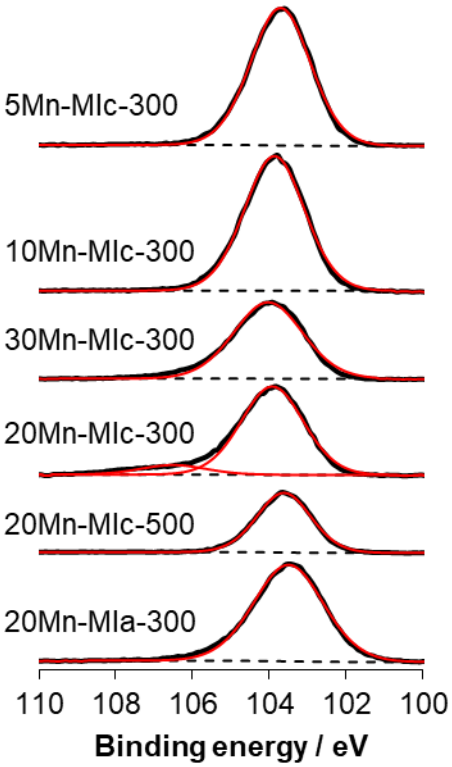

Figure S5. Si 2p XPS signal obtained for MI samples (straight black lines) and components from curve fitting (straight red lines) and background (dotted lines)

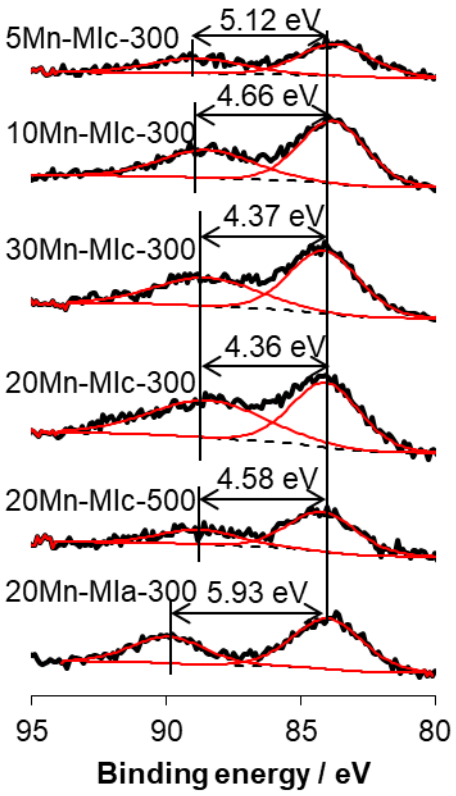

Figure S6. Mn 3s XPS signal obtained for MI samples (straight black lines) and components from curve fitting (straight red lines) and background (dotted lines)

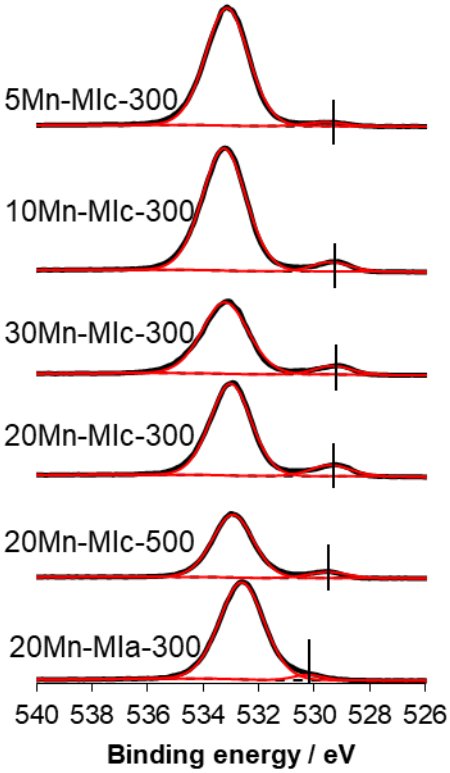

Figure S7. O 1s XPS signal obtained for MI samples (straight black lines) and components from curve fitting (straight red lines) and background (dotted lines)

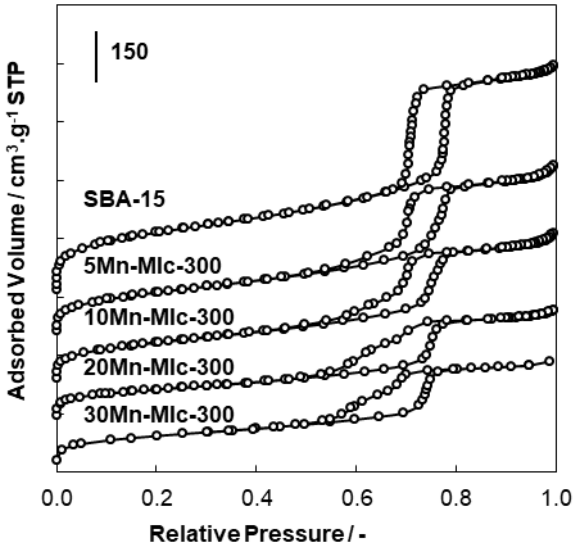

Figure S8. Adsorption/desorption isotherms (shift of 150 $cm^3.g^{-1}$ each) for Mn (5, 10, 20, 30 wt.%) oxides supported on SBA-15

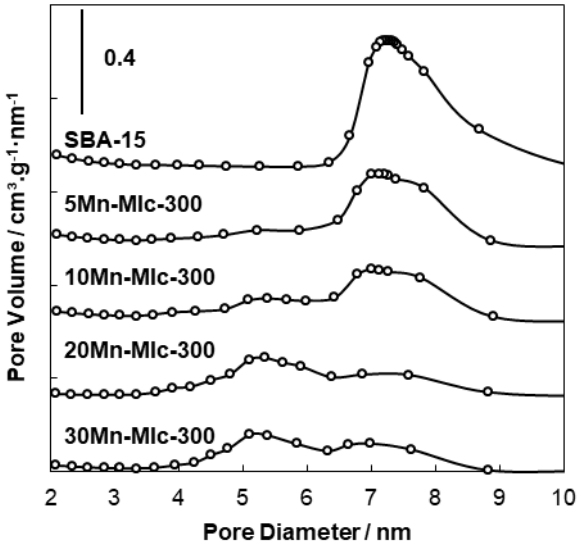

Figure S9. Pore size distribution (shift of 0.4 $cm^3.g^{-1}.nm^{-1}$) for Mn (5, 10, 20, 30 wt%) oxides supported on SBA-15

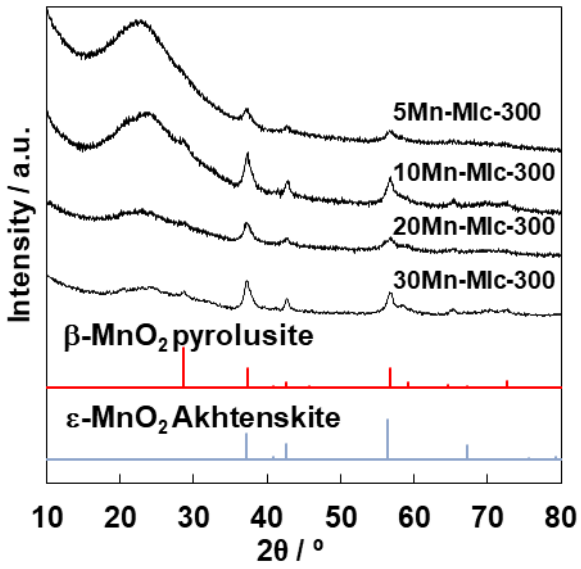

Figure S10. Wide-angle XRD patterns for Mn (5, 10, 20, 30 wt%) oxides supported on SBA-15

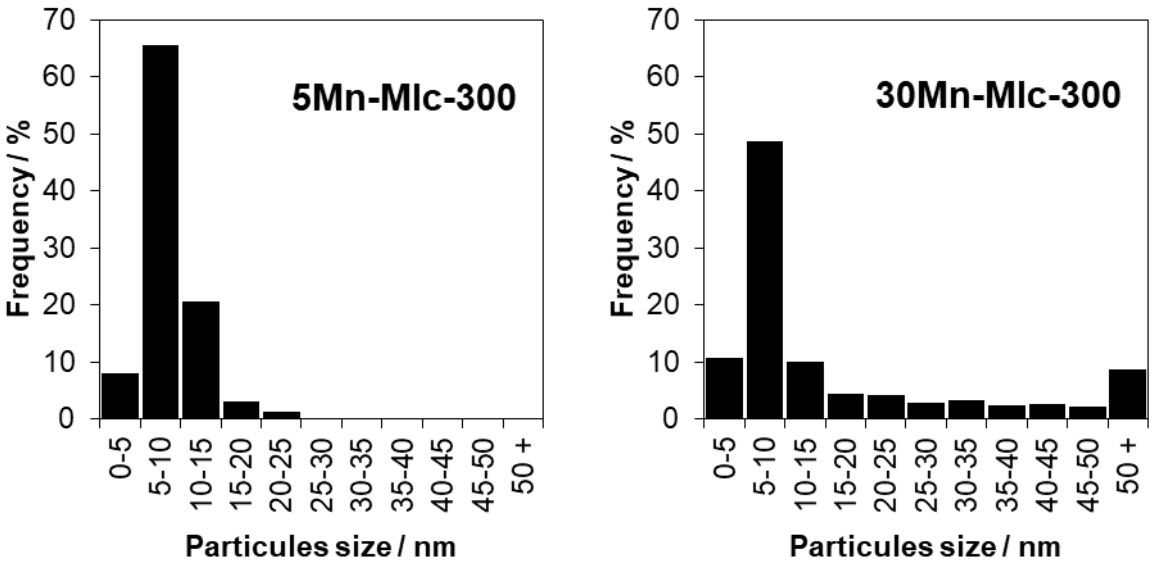

Figure S11. Particles size distribution for Mn (5, 30 wt%) oxides supported on SBA-15

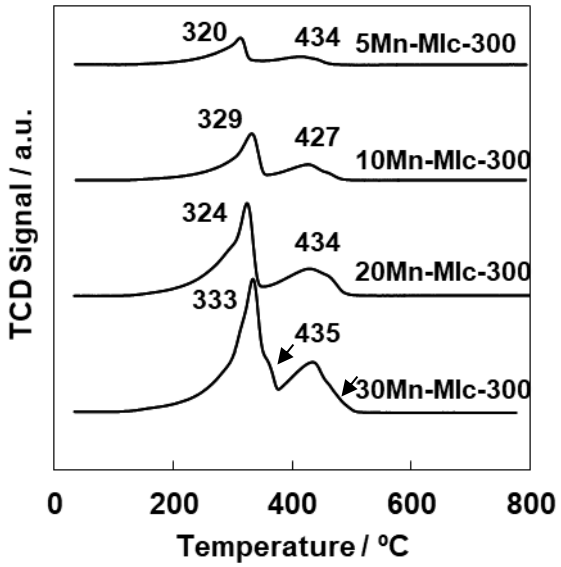

Figure S12. H_2-TPR profiles for Mn (5, 10, 20, 30 wt%) oxides supported on SBA-15

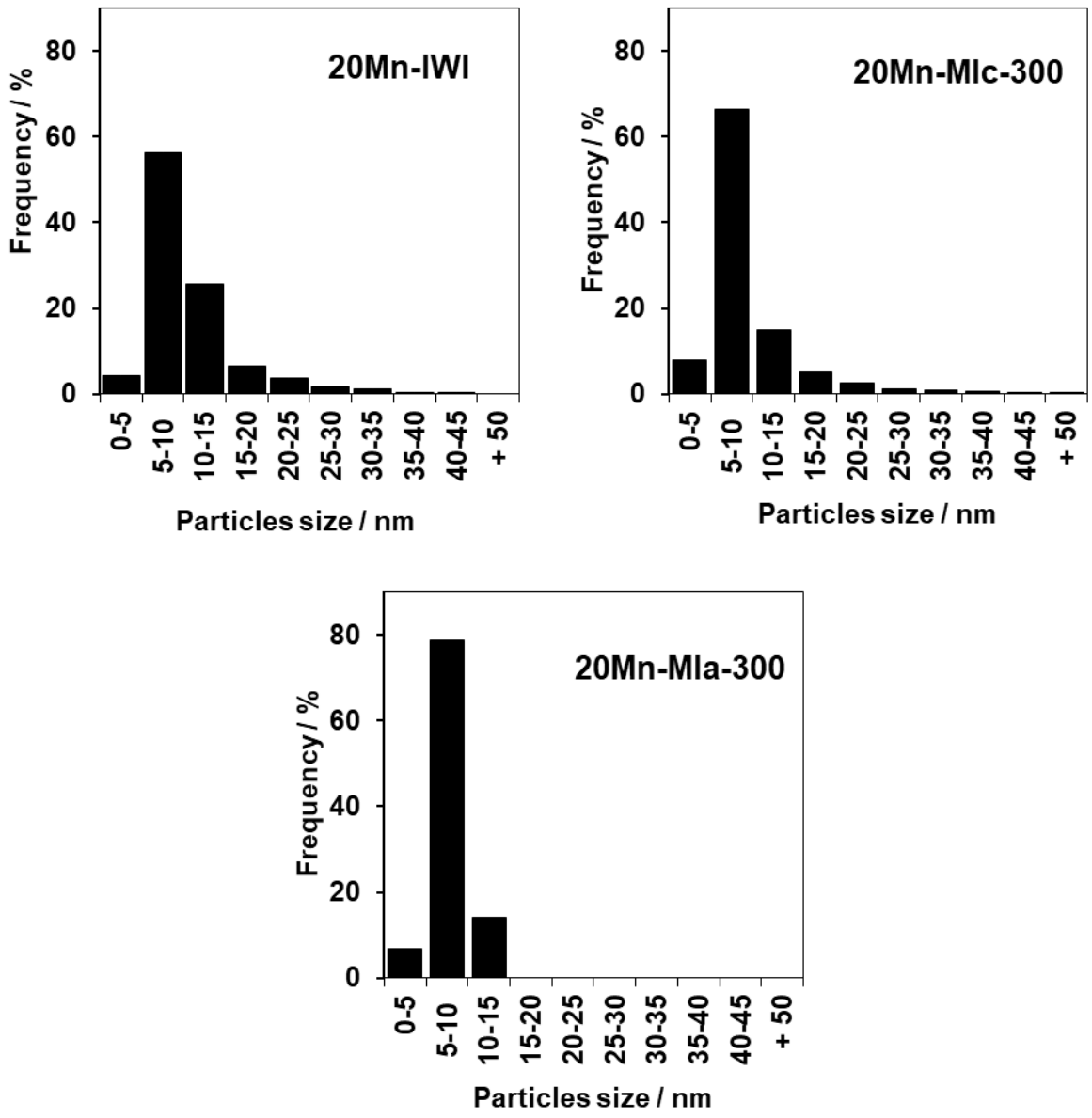

Figure S13. Particles size distribution for Mn (20 wt.%) oxide supported on SBA-15 prepared using different methods

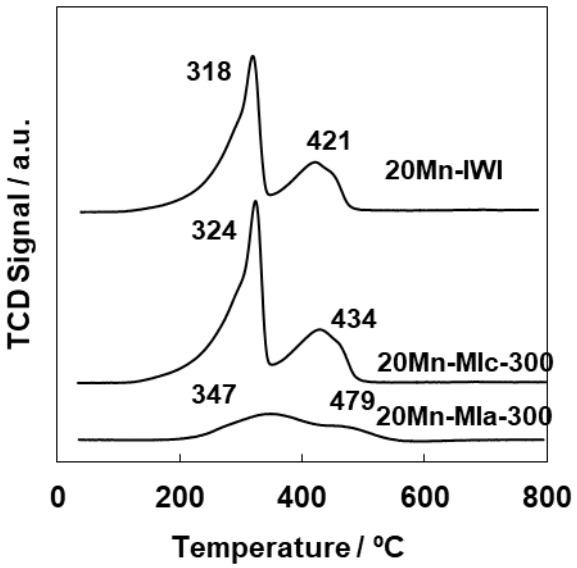

Figure S14. H_2-TPR profiles for Mn (20 wt%) oxide supported on SBA-15 prepared using different methods**.**

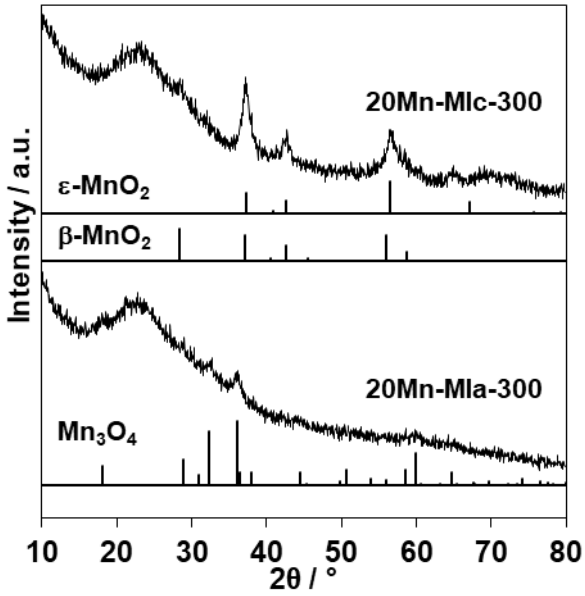

Figure S15. Wide-angle XRD patterns for Mn (20 wt%) oxide supported on SBA-15 prepared using different methods after stabilization test.

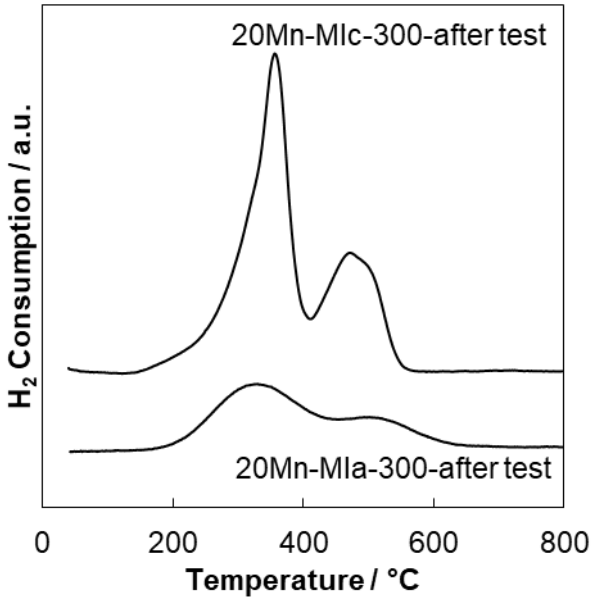

Figure S16. H_2-TPR profiles for 20Mn-MIa-300 and 20Mn-MIc-300 after oxidation tests under dry air. Reaction performed at 170°C

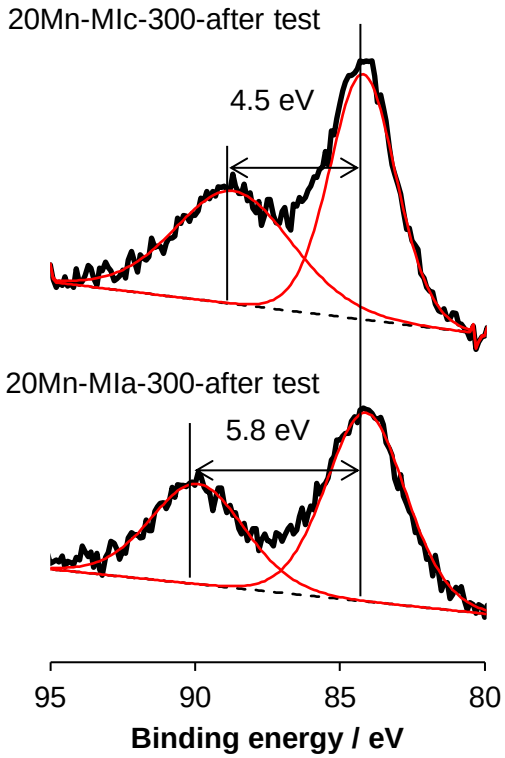

Figure S17. Mn 3s XPS signal (straight black lines) for 20Mn-MIa-300 and 20Mn-MIc-300 after stability tests under dry air (reaction performed at 170°C). Straight red lines: components from curve fitting; Dotted lines: background

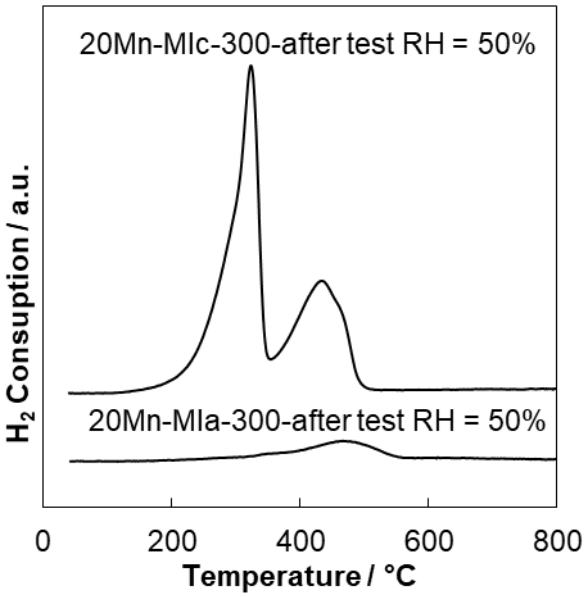

Figure S18. H_2-TPR profiles for Mn (20 wt%) oxide supported on SBA-15 prepared using different methods after oxidation tests. Reaction performed at 130°C at a R.H. of 50% at 25°C.